

Abel inversion using total-variation regularization

T J Asaki¹, R Chartrand², K R Vixie² and B Wohlberg²

¹ Computer and Computational Science Division, CCS-2, MS D413,
Los Alamos National Laboratory, Los Alamos, NM 87545, USA

² Theoretical Division, T-7, MS B284, Los Alamos National Laboratory,
Los Alamos, NM 87545, USA

E-mail: rickc@lanl.gov

Received 2 March 2005, in final form 11 August 2005

Published 10 October 2005

Online at stacks.iop.org/IP/21/1895

Abstract

In the case of radiography of a cylindrically symmetric object, the Abel transform is useful for describing the tomographic measurement operator. The inverse of this operator is unbounded, so regularization is required for the computation of satisfactory inversions. We introduce the use of the total variation seminorm for this purpose, and prove the existence and uniqueness of solutions of the corresponding variational problem. We illustrate the effectiveness of the total-variation regularization with an example and comparison with the unregularized inverse and the H^1 regularized inverse.

(Some figures in this article are in colour only in the electronic version)

1. Abel inversion

Consider a cylindrically symmetric object having cylindrical coordinates $(r, \theta, z) \in [0, R) \times [0, 2\pi) \times (0, L)$. Let $u = u(r, z)$ be the density of the object at (r, θ, z) ; we can regard the domain of u to be $[0, R) \times (0, L)$.

Suppose a radiograph of the object is made by sending parallel beams of radiation through the object, perpendicular to the axis of symmetry. The transmitted radiation is measured by a detector lying in the plane $y = y_0$, where $y_0 > R$. A reasonable model, though oversimplified, is that for each (x, z) the radiograph intensity gives a measure of the attenuation $d(x, z)$ that is the density integral along the line through the object and perpendicular to the detector plane at (x, z) . Then d will be the Abel transform of u , given by

$$Pu(x, z) = 2 \int_{|x|}^R \frac{ru(r, z)}{\sqrt{r^2 - x^2}} dr. \quad (1)$$

See figure 1. As expected, Pu is symmetric about $x = 0$; henceforth we regard the domain of d and Pu to be $U = (0, R) \times (0, L)$. The Abel transform defines a linear operator P on functions

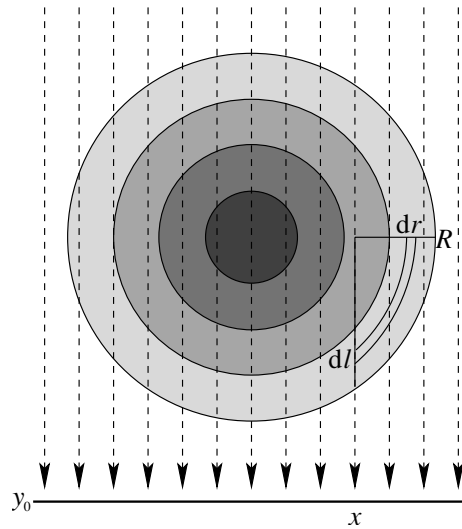


Figure 1. Axial section of a cylindrically symmetric, variable density object. The Abel transform gives the line integral through the object at each point. The infinitesimals are related by $dl = r dr / \sqrt{r^2 - x^2}$.

defined on U . It is an integral operator, with kernel $k(x, r) = \frac{2r}{\sqrt{r^2 - x^2}} \chi_{\{(x,r): x < r\}}$. One easily checks that $\|k(\cdot, r)\|_1 = \pi$ for every r and $\|k(x, \cdot)\|_1 = 2\sqrt{R^2 - x^2} \leq 2R$. Then by a standard result in measure theory (see [1], for example), $\|Pu(\cdot, z)\|_{L^p((0,R))} \leq \pi^{\frac{1}{p}} (2R)^{\frac{1}{q}} \|u(\cdot, z)\|_p$ for $1 \leq p \leq \infty$ and $\frac{1}{p} + \frac{1}{q} = 1$. It follows that P is bounded on $L^p(U)$ and $\|P\| \leq (\pi L)^{\frac{1}{p}} (2R)^{\frac{1}{q}}$.

A left inverse of the Abel transform on L^p is given by

$$P^{-1}v(r, z) = \frac{-1}{\pi r} \frac{d}{dr} \int_r^R \frac{xg(x, z) dx}{\sqrt{x^2 - r^2}}. \quad (2)$$

This can be verified by direct calculation, using the Tonelli–Fubini theorems and the almost-everywhere differentiability of indefinite integrals. Thus P is invertible on its range, and one can, in principle, determine u from d by computing $u = P^{-1}d$ explicitly. However, in practice one finds noise in the data. Computing $u = P^{-1}d$ gives poor results. This is because the operator P^{-1} is unbounded. An example demonstrating this is $v(x, z) = \chi_{(0,a)}(x)$ for arbitrary $a \in (0, R)$. Then $\|v\|_1 = \|v\|_2^2 = aL$, and $P^{-1}v(r, z) = (\pi\sqrt{a^2 - r^2})^{-1} \chi_{(0,a)}(r)$. Since $\|P^{-1}v\|_2 = \infty$ and $\|P^{-1}v\|_1 = \frac{1}{2}$ independently of a , we see that P^{-1} is unbounded on L^2 and L^1 .

1.1. Other methods

Many Abel-inversion techniques have been developed. Several involve fitting functions of a simple form to the data, and then directly inverting the Abel transform. See [2] for a comparison of several methods of this sort. Other approaches involve filtering the data by analysing its Fourier transform (e.g., [3]). Others expand the inverse with respect to a chosen basis, and then determine coefficients by fitting the Abel transform to the data (e.g., [4, 5]).

Such approaches resemble in spirit the application of a lowpass filter to the inverse. A variational approach that does exactly this is H^1 regularization, with which we compare our method in section 4. Our choice of regularization results in an Abel-inversion model that is closely related to the total-variation denoising model of Rudin, Osher and Fatemi [6]. It and H^1 regularization can be regarded as generalizations of Tikhonov regularization [7]. Our method is particularly suitable when u is discontinuous. For another approach to obtaining discontinuous Abel inverses, see [8].

2. Regularization via total cylindrical variation

A more realistic model involves imposing a regularity condition on u , while attempting to keep Pu near d . This can be implemented by minimizing the functional F defined by

$$F(u) = \alpha \int_U |\nabla u(r, z)| r \, dr \, dz + \frac{1}{2} \int_U |Pu - d|^2, \quad (3)$$

where α is a nonnegative tuning parameter. The larger the value of α , the more noise will be removed, at the cost of Pu straying farther from d . Henceforth, we will use r for the first-coordinate function on U .

Defining the first term of $F(u)$ and the domain of F requires some care, as we do not wish to require u to be differentiable, or even continuous. The quantity ∇u is defined in the distributional sense:

$$\int_U |\nabla u| r := \sup \left\{ \int_U u \nabla \cdot (r\varphi) : \varphi \in C_c^1(U)^2, |\varphi| \leq 1 \right\}. \quad (4)$$

Similarly,

$$\int_U |\nabla u| := \sup \left\{ \int_U u \nabla \cdot \varphi : \varphi \in C_c^1(U)^2, |\varphi| \leq 1 \right\}. \quad (5)$$

Note that both (4) and (5) hold by integration by parts when u is smooth.

The L^1 functions u for which the seminorm defined by (5) is finite form the space of functions of bounded variation on U , denoted by $BV(U)$. This space is a Banach space under the norm obtained by adding the L^1 norm:

$$\|u\|_{BV(U)} := \int_U |\nabla u| + \|u\|_{L^1(U)}. \quad (6)$$

One can also isometrically identify the space of functions for which (4) is finite with the cylindrically symmetric functions belonging to $BV(\tilde{U})$, where $\tilde{U} = (0, R) \times [0, 2\pi) \times (0, L)$ is the cylinder determined by U .

3. Existence and uniqueness of minimizer

We will need the following:

Lemma 3.1. *Let $u \in L^1(U)$. Then*

$$\int_U |\nabla u| r \leq \max\{1, R\} \|u\|_{BV(U)}. \quad (7)$$

Proof.

$$\begin{aligned} \int_U |\nabla u| r &= \sup \left\{ \int_U u \nabla \cdot (r \varphi) : \varphi \in C_c^1(U)^2, |\varphi| \leq 1 \right\} \\ &= \sup \left\{ \int_U u (\varphi_1 + r \nabla \cdot \varphi) : \varphi \in C_c^1(U)^2, |\varphi| \leq 1 \right\} \\ &\leq \int_U |u| + R \int_U |\nabla u|. \end{aligned} \quad (8)$$

□

Lemma 3.2. $\|u\|_{L^2(U)} \leq C \|u\|_{BV(U)}$.

Proof. This is a consequence of Poincaré's inequality for BV [9]. If $u \in BV(U)$, then

$$\begin{aligned} \|u\|_2 &\leq \left\| u - \frac{1}{|U|} \int_U u \right\|_2 + \left\| \frac{1}{|U|} \int_U u \right\|_2 \\ &\leq C \int_U |\nabla u| + \frac{1}{\sqrt{|U|}} \int_U |u| \\ &\leq C \|u\|_{BV(U)}. \end{aligned} \quad (9)$$

□

Proposition 3.3. If $d \in L^2$, the functional F defined in (3) is continuous on $BV(U)$.

Proof. Suppose $u_n \rightarrow u$ in $BV(U)$. By the previous lemma, $u_n \rightarrow u$ in $L^2(U)$ also. Since P is continuous on $L^2(U)$, it follows that $\|Pu_n - d\|_2^2 \rightarrow \|Pu - d\|_2^2$.

Since the quantity defined in (4) is a seminorm,

$$\left| \int_U |\nabla u_n| r - \int_U |\nabla u| r \right| \leq \int_U |\nabla (u_n - u)| r \leq \max\{1, R\} \|u_n - u\|_{BV(U)} \rightarrow 0. \quad (10)$$

Thus $F(u_n) \rightarrow F(u)$. □

Because seminorms and affine transformations are convex and squared norms are strictly convex, the functional F is strictly convex. Therefore a local minimum of F will be a global minimum, and a global minimizer will be unique. It remains to prove that such a minimizer exists.

Theorem 3.4. Let $d \in L^2(U)$. Then F has a unique global minimizer on $BV(U)$.

Proof. As explained above, if a minimizer exists it will be unique. Since F is nonnegative valued, choose a sequence $(u_n) \subset BV(U)$ such that $F(u_n) \rightarrow \inf_{u \in BV(U)} F(u)$. Extend each u_n to a cylindrically symmetric function $\tilde{u}_n \in BV(\tilde{U})$. We will show that $\|\tilde{u}_n\|_{BV(\tilde{U})}$ is bounded.

Since $F(u_n)$ is bounded, so is $\int_{\tilde{U}} |\nabla \tilde{u}_n|$, as this is simply $2\pi \int_U |\nabla u_n| r$. This in turn implies that

$$\left\| \tilde{u}_n - \frac{1}{|\tilde{U}|} \int_{\tilde{U}} \tilde{u}_n \right\|_{L^1(\tilde{U})} \quad (11)$$

is bounded by Poincaré's inequality. Thus, the boundedness of \tilde{u}_n in $L^1(\tilde{U})$, and hence in $BV(\tilde{U})$, will follow from the boundedness of the scalar sequence

$$\int_{\tilde{U}} \tilde{u}_n = 2\pi \int_U u_n r. \quad (12)$$

But we also have that $\|Pu_n - d\|_2^2$ is bounded, hence so is $\|Pu_n\|_2$. Since U is a bounded set, $\|Pu_n\|_1$ is bounded as well. A Tonelli–Fubini change of integration order gives us that

$$\begin{aligned} \int_U Pu_n &= \int_0^L \int_0^R \int_x^R \frac{2ru_n(r, z)}{\sqrt{r^2 - x^2}} \, dr \, dx \, dz \\ &= \int_0^L \int_0^R \int_0^r \frac{2ru_n(r, z)}{\sqrt{r^2 - x^2}} \, dx \, dr \, dz \\ &= \pi \int_U u_n r. \end{aligned} \tag{13}$$

Thus

$$\left| \int_U u_n r \right| = \frac{1}{\pi} \left| \int_U Pu_n \right| \leq \frac{1}{\pi} \int_U |Pu_n|, \tag{14}$$

which is bounded. Therefore \tilde{u}_n is bounded in $BV(\tilde{U})$.

The space $BV(\tilde{U})$ is compactly embedded in $L^1(\tilde{U})$ [10]. Hence we can choose a subsequence (\tilde{u}_{n_k}) convergent in $L^1(\tilde{U})$, say to \tilde{u}_0 . Then by the lower semicontinuity of the BV seminorm,

$$\int_U |\nabla u_0| r \leq \liminf \int_U |\nabla u_{n_k}| r. \tag{15}$$

For each $j \in \mathbb{N}$, let $U_j = \{(r, z) \in U : r > \frac{1}{j}\}$, and let $V_j = U_j \setminus \bigcup_{i < j} U_i$. Then

$$\int_{V_j} |u_{n_k} - u_0| \leq j \int_U |u_{n_k} - u_0| r = \frac{j}{2\pi} \int_{\tilde{U}} |\tilde{u}_{n_k} - \tilde{u}_0| \rightarrow 0. \tag{16}$$

Thus $u_{n_k} \rightarrow u_0$ in $L^1(V_j)$, so Pu_{n_k} converges to Pu_0 in measure on V_j . Then by a version of Fatou’s lemma, $\int_{V_j} |Pu_0 - d|^2 \leq \liminf \int_{V_j} |Pu_{n_k} - d|^2$. Thus

$$\begin{aligned} \int_U |Pu_0 - d|^2 &= \sum_j \int_{V_j} |Pu_0 - d|^2 \leq \sum_j \liminf \int_{V_j} |Pu_{n_k} - d|^2 \\ &\leq \liminf \sum_j \int_{V_j} |Pu_{n_k} - d|^2 = \liminf \int_U |Pu_{n_k} - d|^2. \end{aligned} \tag{17}$$

This and (15) imply that $F(u_0) \leq \liminf F(u_{n_k}) = \inf_{u \in BV(U)} F(u)$. Thus u_0 is a global minimizer of F . \square

4. Computational considerations

In order to compute the minimizer of F , it is useful to calculate the derivative of F . Let $u, v \in BV(U)$. Calculating formally, we find that the directional derivative of F at u in the direction of v is

$$D_v F(u) = \alpha \int_U \frac{\nabla u}{|\nabla u|} r \cdot \nabla v + \int_U (Pu - d) P v. \tag{18}$$

This makes sense if u is smooth and $\nabla u \neq 0$ almost everywhere. Under such assumptions, we may proceed further and isolate v :

$$\begin{aligned} D_v F(u) &= -\alpha \int_U \nabla \cdot \left(r \frac{\nabla u}{|\nabla u|} \right) v + \int_U P^*(Pu - d)v \\ &= \left\langle -\alpha \left(\frac{\partial u}{\partial r} \frac{r}{|\nabla u|} + r \nabla \cdot \frac{\nabla u}{|\nabla u|} \right) + P^*P - P^*d, v \right\rangle_2. \end{aligned} \tag{19}$$

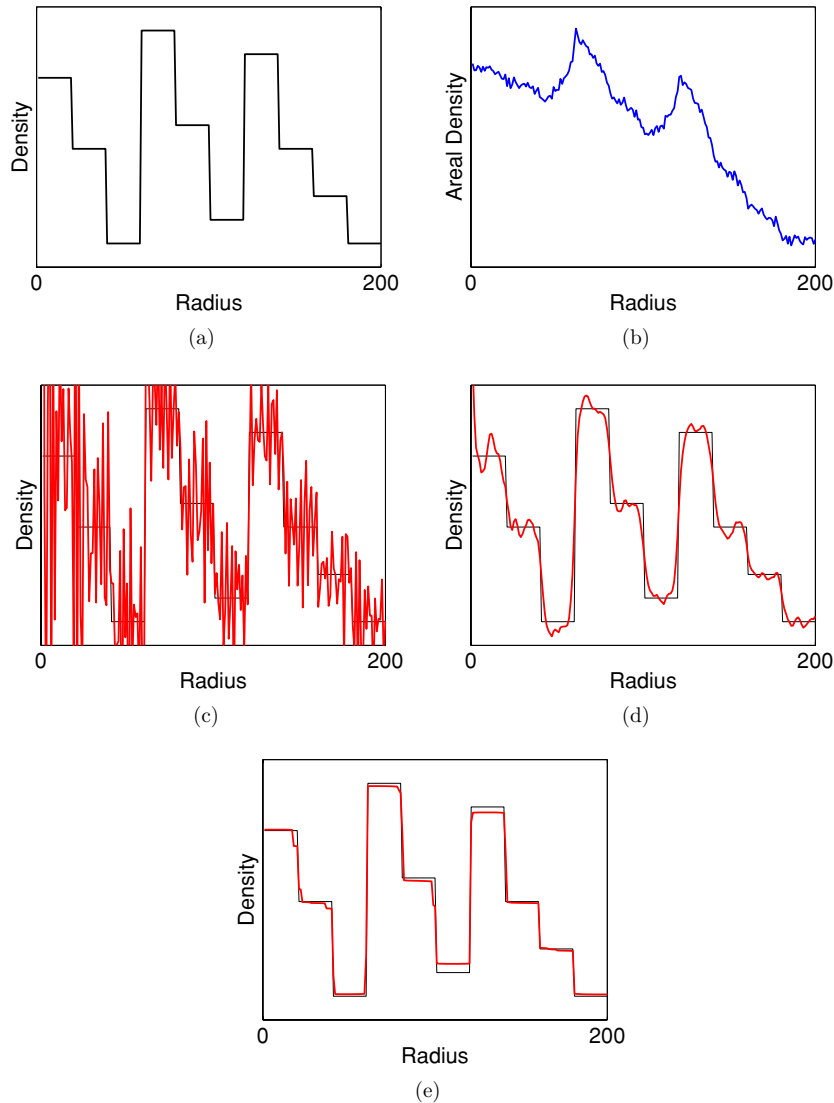


Figure 2. (a) Density profile; (b) Abel transform, with noise added; (c) unregularized Abel inversion; (d) H^1 -regularized Abel inversion; (e) TV -regularized Abel inversion.

This says that for such u , F has a Gateaux derivative:

$$F'(u) = -\alpha \left(\frac{\partial u}{|\nabla u|} + r \nabla \cdot \frac{\nabla u}{|\nabla u|} \right) + P^* P u - P^* d. \tag{20}$$

A commonly used procedure for computing the minimum of functionals is gradient descent, which amounts to introducing an artificial time variable and numerically solving the PDE $u_t = -F'(u)$. Several issues present themselves. One is the smoothness of u required for $F'(u)$ to make sense. However, it is well known that any BV function u can be approximated arbitrarily well by C^∞ functions (u_n), in the sense that $u_n \rightarrow u$ in L^1 and $\|u_n\|_{BV} \rightarrow \|u\|_{BV}$. (Having $\|u_n - u\|_{BV} \rightarrow 0$ is not possible in general.) A second issue

Table 1. Mean-squared difference between the object of figure 2 and the regularized reconstruction, for various multiples of the regularization parameter chosen by the discrepancy principle.

Factor	Mean-squared error $\times 1000$	
	H^1	TV
0.25	9.94	2.30
0.5	6.79	1.00
0.75	6.06	1.02
0.9	5.93	1.06
1.0	5.89	1.11
1.1	5.89	1.18
1.25	5.91	1.30
1.5	6.01	1.58
1.75	6.14	1.93
2.0	6.29	2.33

is that in general $F'(u) \notin BV(U)$; rather, $F'(u) \in BV(U)^*$. Thus, it is not clear how to make sense of an evolution of the form $u_{n+1} = u_n - \Delta t F'(u_n)$. However, thinking in terms of a numerical implementation on an $m \times n$ grid, one can regard F to be defined on the finite-dimensional space \mathbb{R}^{mn} instead of the infinite-dimensional space $BV(U)$. Then one has $F'(u) \in (\mathbb{R}^{mn})^* = \mathbb{R}^{mn}$ as well. The theory developed above does not directly apply to this setting, but in practice one tends to obtain at least approximate convergence to an approximate minimizer. A third issue with gradient descent is that even when convergence occurs, it tends to occur slowly. For this reason, we sought alternatives to gradient descent.

We use the lagged-diffusivity fixed-point method of Vogel and Oman [11]. Global, linear convergence of the method is proven in [12]. The iteration used is a discretization of the equation

$$u_{n+1} = u_n - (P^*P + \alpha L)^{-1}(P^*Pu_n - P^*d + \alpha Lu_n), \quad (21)$$

where

$$L = 2\pi r \nabla \cdot \frac{\nabla}{|\nabla u_n|} + 2\pi \frac{\partial}{\partial r} \frac{1}{|\nabla u_n|}. \quad (22)$$

In particular, $|\nabla u|$ is discretized in the regularized form $\sqrt{|\nabla u|^2 + \beta}$ for a small constant β , to avoid singularities. For more details of the implementation, see [13].

An example using a simulated two-dimensional object is presented in figure 2. An axial section of the density function u is shown in figure 2(a). A simulated radiograph is obtained by computing the Abel transform of u and adding Gaussian noise of variance equal to 1.5% of the largest data value. The result is shown in figure 2(b). Figure 2(c) shows the unsatisfactory result of computing the inverse Abel transform of the noisy data.

We compare the results of regularizing the Abel inversion using (3) with that of regularization with an H^1 penalty term. That is, the quantity $|\nabla u|$ in (3) is replaced with $|\nabla u|^2$. In both cases, the regularization parameter α is chosen according to the discrepancy principle: the resulting minimizer u should be such that the mean-squared discrepancy between Pu and d should equal the variance of the noise in d . This reflects the principle that of the many solutions to an ill-posed inverse problem that are consistent with the data, the solution that should be chosen is the one that is most regular. The noise variance is not generally known in practice, so we estimate the noise variance by comparing d with a smoothed version of d .

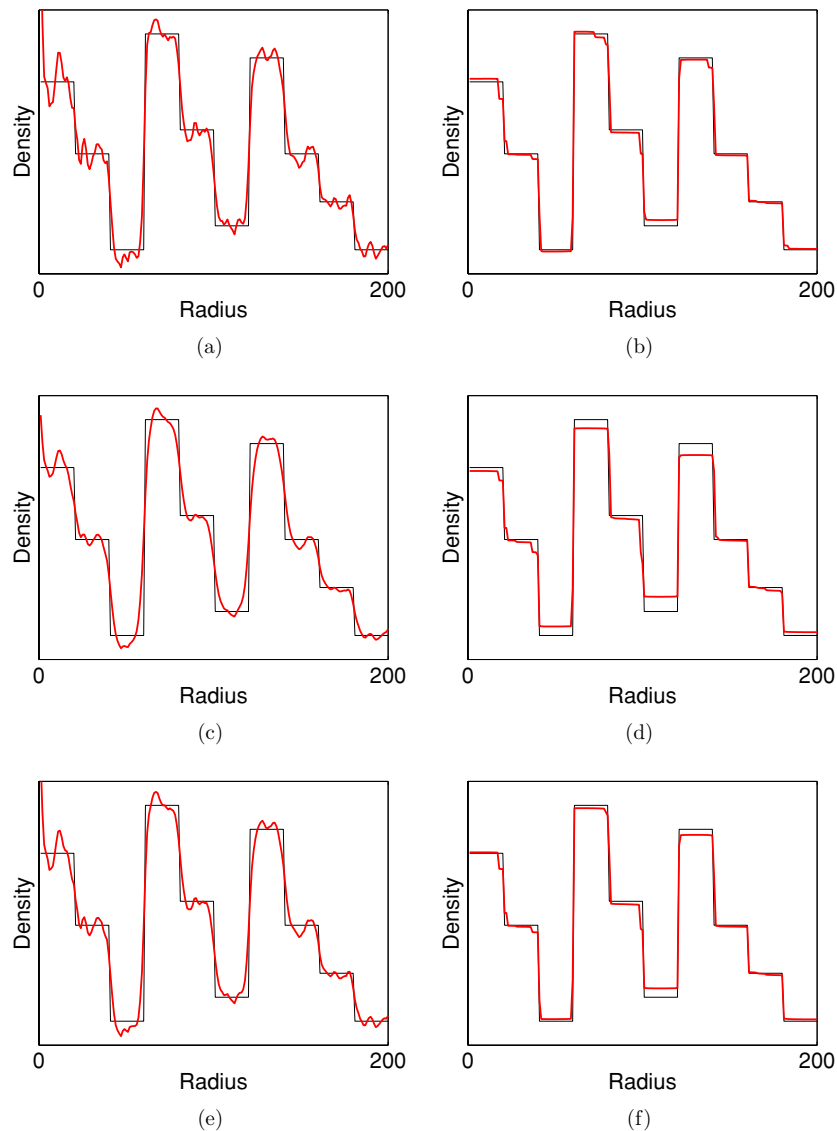


Figure 3. (a) Underregularized H^1 Abel inversion; (b) underregularized TV Abel inversion; (c) overregularized H^1 Abel inversion; (d) overregularized TV Abel inversion; (e) correctly regularized H^1 Abel inversion; (f) correctly regularized TV Abel inversion.

In the example, we estimated the noise variance to be 7.715, while the actual variance of the noise was 7.261. The values of α resulting from the discrepancy principle were $\alpha_{H^1} = 32.54$ for the H^1 regularization and $\alpha_{TV} = 9.644$ for the total-variation regularization. Figure 2(d) shows the result of the H^1 regularization. The result is a smooth inverse, but important edge information is lost. This is because the H^1 seminorm is infinite for functions with a jump discontinuity. Our total-variation regularized Abel inverse is shown in figure 2(e). The reconstruction preserves edges and is smooth between them. The mean-squared difference between the reconstructed u and the known object density was 0.005 89 in the case of the H^1 regularization, and 0.001 11 in the case of total-variation regularization.

We also examine the result of different parameter choices. Table 1 shows the mean-squared difference between the object pictured in figure 2(a) and the reconstructed object, for various multiples of the parameters chosen above. Figure 3 shows the results for factors of 0.5, 2.0 and 1.0. For the H^1 regularization, the mean-squared error is least for $\alpha \approx \alpha_{H^1}$. For total-variation regularization, the mean-squared error is least for $\alpha \approx 0.5\alpha_{TV}$, suggesting that the parameter choice above results in over-regularization. However, in figure 3 we see that the choice of $\alpha = \alpha_{TV}$ gives better preservation of the edges and the geometric nature of the object. We also note that computing these mean-squared errors is not normally possible in practice, as the ‘true’ object will not generally be available.

Acknowledgments

The work of all authors was performed under the auspices of the Department of Energy under contract W-7405-ENG-36.

References

- [1] Conway J B 1990 *A Course in Functional Analysis* (New York: Springer) p 28
- [2] Cremers C J and Birkebak R C 1966 Application of the Abel integral equation to spectroscopic data *Appl. Opt.* **5** 1057–64
- [3] Smith L M, Keefer D R and Sudharsanan S I 1988 Abel inversion using transform techniques *J. Quant. Spectrosc. Radiat. Transfer* **39** 367–73
- [4] Maldonado C D, Caron A P and Olsen H N 1965 New method for obtaining emission coefficients from emitted intensities: I. Circularly symmetric light sources *J. Opt. Soc. Am.* **55** 1247–54
- [5] Pretzler G 1991 A new method for numerical Abel-inversion *Z. Naturforsch. A* **46** 639–41
- [6] Rudin L, Osher S and Fatemi E 1992 Nonlinear total variation based noise removal algorithms *Physica D* **60** 259–68
- [7] Tikhonov A N 1963 Regularization of incorrectly posed problems *Sov. Math. Dokl.* **4** 1624–27
- [8] Cheng J, Hon Y C and Wang Y B 2004 A numerical method for the discontinuous solution of Abel integral equations *Inverse Problems and Spectral Theory* (Providence, RI: American Mathematical Society) p 233
- [9] Ambrosio L, Fusco N and Pallara D 2000 *Functions of Bounded Variation and Free Discontinuity Problems* (Oxford: Oxford University Press) p 152
- [10] Evans L C and Gariepy R F 1992 *Measure Theory and Fine Properties of Functions* (Boca Raton, FL: CRC Press) p 176
- [11] Vogel C R and Oman M E 1996 Iterative methods for total variation denoising *SIAM J. Sci. Comput.* **17** 227–38
- [12] Chan T F and Mulet P 1999 On the convergence of the lagged diffusivity fixed point method in total variation image restoration *SIAM J. Numer. Anal.* **36** 354–67
- [13] Asaki T J, Campbell P R, Chartrand R, Powell C, Vixie K R and Wohlberg B 2005 Total-variation regularized Abel inversions: applications *Preprint LA-UR-05-2657*